SPACE WEATHERING PROCESSES ON MERCURY S. K. Noble and C. M. Pieters, Brown University. Dept of Geological Sciences, Providence RI 02912. noble@porter.geo.brown.edu

Introduction: Like the Moon, Mercury has no atmosphere to protect it from the harsh space environment and therefore it is expected that it will incur the effects of space weathering [1]. These weathering processes are capable of both creating regolith and altering its optical properties [1,2,3]. However, there are many important differences between the environments of Mercury and the Moon. These environmental differences will almost certainly affect the weathering processes as well as the products of those processes. It should be possible to observe the effects of these differences in Vis/NIR spectra of the type expected to be returned by MESSENGER. More importantly, understanding these weathering processes and their consequences is essential for evaluating the spectral data returned from MESSENGER and other missions in order to determine the mineralogy and the iron content of the Mercurian surface. Theoretical and experimental work has been undertaken in order to better understand these consequences [4,5].

Mercurian Environment: Due to its higher impactor flux and greater density, Mercury will produce 13.5 times the melt and 19.5 times the vapor than is produced on the Moon per unit area [6]. Additionally, Mercury has a magnetic field that protects its surface from charged particles which severely reduces the solar wind flux at the surface [7]. Therefore, melting and vaporization due to micrometeorites are expected to dominate space weathering on Mercury with little or no solar wind sputtering effects [1]. Furthermore, agglutinitic glass-like deposits and vapor deposited coatings should be created faster and more efficiently on Mercury. The Mercurian environment is also notable for its extreme temperature range. Due to its slow rotation and proximity to the sun, equatorial regions of Mercury achieve temperatures above 700K during the day, while nighttime temperatures fall below 100K.

The nanometer-scale metallic Fe particles ($npFe^0$) that are ubiquitous in the rims and agglutinates of lunar soil [8] (figure 1) should also be present on Mercury. Even for the endmember case where the surface of Mercury has no native FeO, the iron brought in by meteorites should be sufficient to make the formation of $npFe^0$ through vapor fractionation an important process on the planet. Amounts as small as 0.05 wt % $npFe^0$ are enough to affect the optical properties [2].

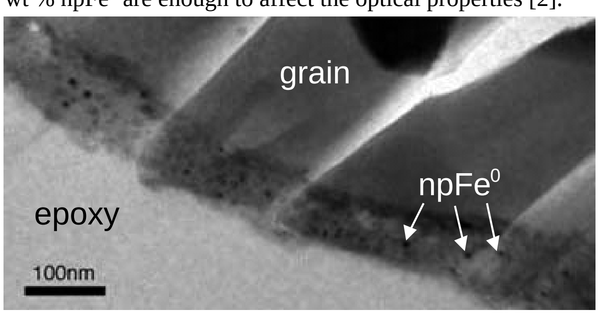

Figure 1. TEM bright field image of $npFe^0$-rich rim on a lunar soil grain.

Size of $npFe^0$ Particles: The size distribution of metallic Fe particles in a soil strongly controls the optical effects on the Vis/NIR spectrum. In lunar rims, these $npFe^0$ particles range from ~1-12nm in dia. with an average of ~3nm [9]. The smallest particles (3-5nm) will tend to redden the soil while larger particles (>10nm) will simply cause darkening [9,10].

Ostwald Ripening: In figure 2 are shown the results of a $npFe^0$ study in which Fe^0 particles averaging about 8 nm in diameter were created and then heated for 10 hours at a range of temperatures [12]. The graph plots the final size of the particles vs. the heating temperature. This study is not directly applicable to Mercury because here iron particles are in grain to grain contact rather than occurring as isolated particles suspended in a glass matrix as in space weathering products. However, the experiment is useful because it demonstrates that this size of nanophase Fe^0 particles may only be stable to about 200°C. The majority of Mercury's surface reaches daytime temperatures significantly above 200°C. In fact, during the course of a Mercurian day, the soil at the hottest parts of Mercury will stay above 400°C for about 2 weeks. This increased temperature may be enough to allow the $npFe^0$ particles to grow significantly via Ostwald ripening, a process well known in material sciences [11]. Ostwald ripening is a process by which $npFe^0$ particles in a glass matrix will tend to coarsen due to differences in free energy between curved surfaces.

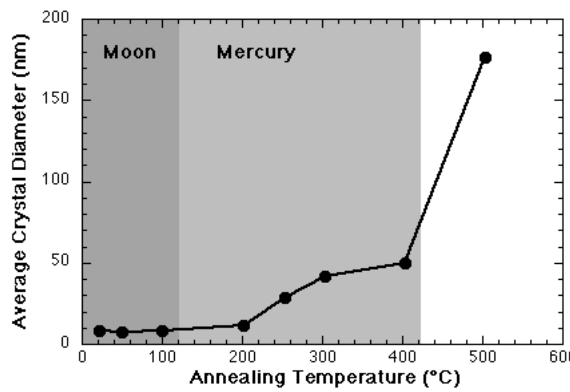

Figure 2. Size of $npFe^0$ particles after annealing for 10 hours. Modified from Glieter, 1989 [12]. The shaded areas show the upper extent of the temperature regimes for the Moon and Mercury, respectively.

A vapor deposition experiment of Hapke *et al.* [13] demonstrated that heating $npFe^0$-rich vapor coatings to a temperature of 650°C for just one hour is sufficient to remove a ferromagnetic resonance. This is hypothesized to occur because particles of $npFe^0$ have grown to be larger than the range that is measured by FMR techniques [4 - 33 nm in dia.[14]]. Thus, it appears that even for $npFe^0$ particles suspended in a glass matrix, increased temperatures can result in significant grain growth.

Determining the rate of Ostwald ripening on Mercury is difficult due to a lack of directly relevant experimental data. The least constrained, and most important, variables are the diffusion coefficient of Fe^0 into the glass matrix, which is strongly temperature dependent, and the surface energy (i.e. boundary between $npFe^0$ and matrix), also somewhat temperature dependent. By considering a wide range of values for these, we have attempted to bound the possible range of grain growth through time that might occur on Mercury (figure 3).

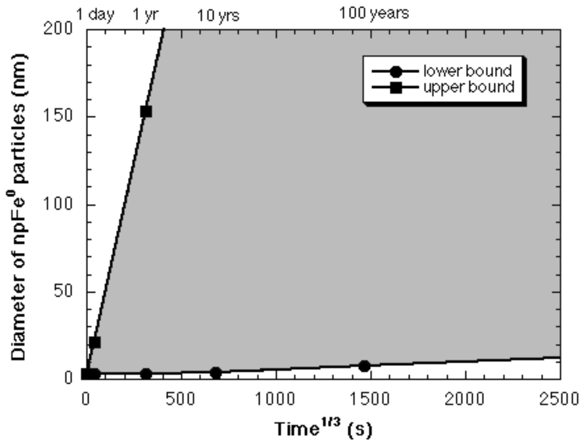

Figure 3. Possible range of effects of Ostwald ripening with time near the equator of Mercury. Lower bound assumes D (diffusion coef.) =10^{-19} m^2/s, σ (surface energy) =0.1 mJ/m^2, Upper bound assumes D=10^{-17} m^2/s, σ =100 mJ/m^2.

Obviously, these results cover a wide range of possibilities, however, even our most conservative estimates (lower bound) indicate that Ostwald ripening should have a significant effect on equitorial Mercurian soils, doubling the size of the $npFe^0$ in a matter of centuries. Of course, with increasing latitude, less solar heating occurs and the thermal regime becomes much more lunar-like where Ostwald ripening will have little to no effect. Certainly polar regions that do not reach temperatures above 200°C (beyond 75°N or S for the hot poles, and 65° for the warm poles) are not expected to be affected by Ostwald ripening as $npFe^0$ particles appear to be stable at those temperatures [12].

Discussion: The size of $npFe^0$ particles will be reflected in remotely acquired data. Ostwald ripening should result in larger Fe^0 particles, on average, near the equator where the highest temperatures are reached. As noted earlier, small $npFe^0$ particles cause reddening of the reflectance spectrum and larger particles result in darkening. If Ostwald ripening dominates over $npFe^0$ production near the equator, we expect the spectral continuum to become darker at lower latitudes as one approaches the equator and the increased heat allows for larger $npFe^0$ particles. The continuum should be reddest at high latitudes, where Ostwald ripening has little or no effect and $npFe^0$ particles remain small.

Our current spectral data set for Mercury, is limited. Most of our spectral data is telescopic [15], largely providing an integrated disk view, masking possible latitudinal variations, as well as regional differences. Also hidden are maturity differences that might be expected at young craters. Two bands of spectral data taken during the Mariner 10 flyby confirms that spectral differences exist on regional and local scales [16], however this dataset does not have the spectral or spatial resolution necessary to see the effects discussed above. Recently, the surface was mapped over the wavelength range 550-940 nm at roughly 200 km resolution by the Swedish Vacuum Solar Telescope [17]. Originally, latitudinal variations were removed in the calibration of this dataset, however, some of the data has been reprocessed to allow spectral variations with latitude to be observed [18] (figure 4). Despite significant scatter, it does appear that, as predicted, there is a positive correlation between spectral redness and increasing latitude.

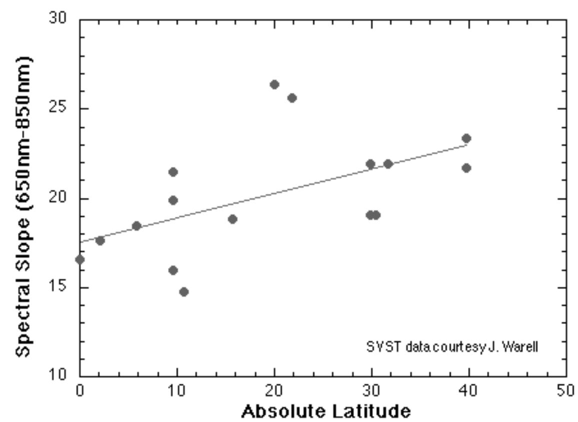

Figure 4. Spectral slope from 650 to 850nm vs. absolute latitude for 16 features on Mercury. Reprocessed Mercury data provided by J. Warell.

Future Work: To address some of the questions raised here more quantitatively, we have begun two sets of experiments. Both use porous silica gel powders impregnated with nanophase metallic iron, following the technique of Allen *et al* [19]. The first of these experiments will investigate the optical effects of particle size of $npFe^0$. Because the pore size, and by analogy the $npFe^0$ particle size, can be controlled, these powders are well suited for studying the optical properties of differing sizes of $npFe^0$ particles. We expect to derive from this experiment the particle size at which $npFe^0$ transitions from causing spectral reddening to darkening. The second experiment involves heating the $npFe^0$-bearing powders for extended periods of time (days to weeks) and measuring the growth rate of the $npFe^0$ particles. This will allow us to better constrain the range of expected effects of Ostwald ripening. In combination, these experiments will provide a foundation for understanding the optical effects of $npFe^0$ in Mercury's environment. This knowledge, in turn, is essential to evaluate mineralogy and iron content from the Vis/NIR spectra expected to be obtained by MESSENGER.

References: [1] Hapke B. (2001) *JGR,* **106**, 10039-10073. [2] Noble S. K. *et al* (2001) *Meteoritics & Planet. Sci.,* **36**, 31-42. [3] Pieters C. M. *et al* (2000) *Meteoritics & Planet. Sci.*, **35**, 1101-1107. [4] Noble S. K. and Pieters C. M. (2001) *Mercury Workshop*, 68-69. [5] Noble S. K. and Pieters C. M. (2002) Astron. Vestnik, submitted. [6] Cintala M. J. (1992) *JGR*, **97**, 947-973. [7] Hartle R. *et al* (1975). *JGR*, **80**, 3689-3693. [8] Keller L. P. and Clemett S. J. (2001) *LPSCXXXII*, ab# 2097. [9] Keller L. P. *et al* (1998) *New Views of the Moon*, 41. [10] Britt D. T. and Pieters C. M. (1994) *GCA*, **58**, 3905-3919. [11] Lifshitz I. M. and Slyozov V. V. (1961) *J. Phys. Chem. Solids*, **19**, 35-50. [12] Gleiter H. (1989) *Progress in Mat. Sci.*, **33**, 223-315. [13] Hapke B. *et al.* (1994) Science, **264**, 1779-1780. [14] Housley R. M. *et al* (1976) PLPSC 7th, 13-26. [15] Vilas F. (1988) Mercury, Univ. of AZ Press, 59-76. [16] Robinson M. S. and Lucey P. G. (1997) *Science*, **275**, 197-199. [17] Warell J. and Limaye S. S. (2001) *Planet. Space Sci.*, 49, 1531-1552. [18] Warell, J. (2002) Personal Communication. [19] Allen C. C. *et al* (1996) *LPSCXXVII*, 13-14.

Acknowledgments: The guidance of Yan Liang and Paul Hess is much appreciated. NASA support (NAG5-4303) is gratefully acknowledged.